

Oscillatory dynamics of a nonlinear amplifier in the high-gain regime: Exploiting a global connection

K. Wiesenfeld*

School of Physics, Georgia Institute of Technology, Atlanta, Georgia 30332

A. R. Bulsara[†] and M. E. Inchiosa[‡]

Space and Naval Warfare Systems Center, San Diego, Code D364, San Diego, California 92152-5001

(Received 21 June 2000)

We study the oscillator equations describing a type of nonlinear amplifier, exemplified by a two-junction superconducting quantum interference device. Just beyond the onset of spontaneous oscillations, the system is known to show significantly enhanced sensitivity to very weak magnetic signals. The global phase-space structure allows us to apply a center manifold technique to calculate the frequency of spontaneous oscillations as a function of the natural control parameters. The derived scaling form compares very well with numerical simulations. The ability to quantify the oscillation frequency permits its exploitation as a detection/analysis tool in remote sensing applications, and could also provide a pathway to a dynamic lowering of the low-frequency noise floor in oscillators exhibiting this class of dynamical behavior.

Nonlinear dynamical systems are very sensitive to small perturbations close to the onset of a bifurcation. This is responsible for the enhanced difficulty in screening out unwanted environmental perturbations near bifurcation points, as observed in experiments of virtually all types, ranging from electrical to mechanical, optical, and fluid systems.¹ Yet, this very same sensitivity affords a general mechanism for signal amplification for a broad class of nonlinear devices.²

A rather different mechanism which can improve a system's sensitivity to weak signals is stochastic resonance (SR).³ Recently, there has been progress towards exploiting the SR effect in dc superconducting quantum interference devices (SQUID's), to take advantage of the background noise rather than devise ever more sophisticated shielding and cancellation mechanisms.⁴ Experiments are underway to carry out this scheme in high- T_c SQUID arrays. These developments are driven by the SQUID's role as the most sensitive detector of magnetic fields, whose practical applications are usually noise limited.⁵ These devices are expected to find increasing utility in a variety of remote sensing applications in areas as diverse as biomagnetics, geophysics, mine/explosive detection, and fundamental measurements.

The dc SQUID consists of two Josephson junctions symmetrically inserted into a superconducting loop.⁶ In the absence of external signals, it exists in either a static (superconducting) or a dynamic (finite voltage) state, depending on biasing. As with many physical systems, the dynamics follow the "particle-in-a-potential" paradigm, with the potential function having multiple stable minima in the static case. In this state, the dynamical variables (the Schrödinger phase angles) converge to constant values at long times. As a parameter is varied through a bifurcation point, the potential minima disappear and the system is attracted to a periodic orbit, corresponding to oscillatory solutions for the phase angles modulo 2π or the experimentally observable circulating current.⁷ Recent experiments and simulations^{4,8} show that the best response to an input signal (in the presence of a

background noise floor) is obtained just past the bifurcation point, where one observes very sensitive input signal dependence of the solutions (i.e., high gain). It is thus of special significance to understand and quantify the dynamics in this regime.

In this paper, we present an analytic calculation of the spontaneous oscillation frequency and its scaling in terms of the (control) parameter "distance" from the singular point. Close to the singular point there is a well-defined separation of time scales which can be exploited using a center manifold technique to reduce the effective phase-space dimension. That we can apply the technique here is somewhat unusual, and is possible only because of the global structure of the dynamics. In particular, the phase-space topology induces a *saddle-node connection*,^{9,10} so that the normally "inaccessible" running state regime—inaccessible in the sense of direct analytic treatment—is rendered accessible, at least close enough to the bifurcation point.

Previous theoretical work has afforded a good description of various other properties of the SQUID dynamics in the static¹¹ and running¹² regimes. Our goal here is to determine explicitly the oscillation frequency, which is related to the voltage across the device,^{6,7} in terms of the bias parameters. Knowing the frequency affords the possibility of dynamically lowering the low-frequency noise floor by injecting a bias signal at this frequency or one of its overtones. Quantifying small changes in the frequency that occur in the presence of external (target) signals could afford a detection mechanism, and experiments involving synchronization to an external signal or to another SQUID would inevitably benefit from an *a priori* knowledge of the oscillation frequency in terms of the bias parameters.

The SQUID dynamics are described by equations for the Schrödinger phases of the (assumed identical) Josephson junctions:^{6,8} $\tau \dot{\delta}_i = I_b/2 + (-1)^i I_s - I_0 \sin \delta_i$, $i = 1, 2$, where I_s , the circulating current induced in the loop by an external magnetic flux, can be written in the form $\beta I_s / I_0 = \delta_1 - \delta_2$

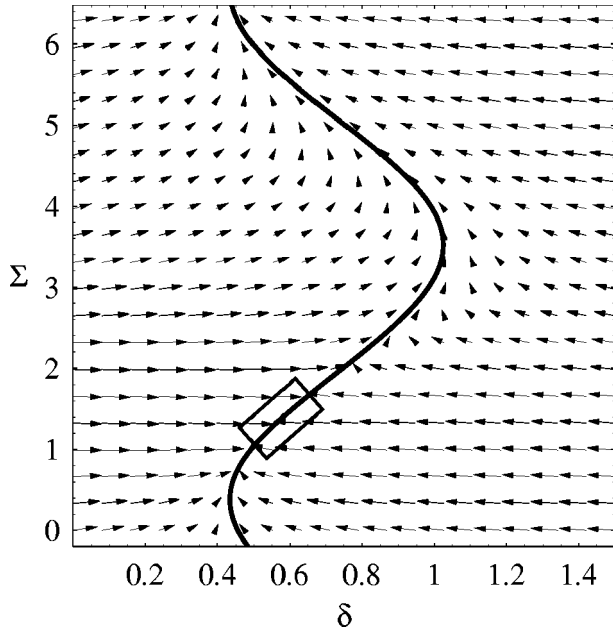


FIG. 1. Phase portrait for the SQUID system. Close to the bifurcation point $J=J_c$ all orbits are attracted on a fast time scale to the one-dimensional subspace (bold); evolution along the center manifold is slow (note that the length of an arrow's tail is proportional to the local flow rate). The local analysis Eq. (2) only describes the boxed region, but this captures the main contribution to the total period of the running state when $J>J_c$. The plot shown is for $\Phi_{ex}=0.2$, $\beta=1$, and $J-J_c=0.007$.

$-2\pi\Phi_e/\Phi_0$. Here, $\tau=\hbar/(2eR)$ is a characteristic time constant (R being the normal state resistance of the junctions), $\beta=2\pi LI_0/\Phi_0$ the nonlinearity parameter, L the loop inductance, I_0 the junction critical current, and $\Phi_0\equiv h/(2e)$ the flux quantum. The two natural experimental control parameters are the applied dc magnetic flux Φ_e and the dc bias current I_b , which we take to be symmetrically applied to the loop. It is convenient to introduce a scaled time, flux ($\Phi_{ex}\equiv\Phi_e/\Phi_0$), and current [$J\equiv I_b/(2I_0)$], and to rewrite the differential equations in terms of the sum and difference variables,^{6,13,14} $\Sigma\equiv(\delta_1+\delta_2)/2$, $\delta\equiv(\delta_1-\delta_2)/2$, with the result (defining $a\equiv\pi\Phi_{ex}$),

$$\dot{\delta} = -\frac{2}{\beta}(\delta-a) - \cos\Sigma \sin\delta$$

$$\dot{\Sigma} = J - \cos\delta \sin\Sigma. \quad (1)$$

The key qualitative feature of the dynamics is illustrated in the phase-space portrait of Fig. 1. In the superconducting regime, the system is attracted to a stable fixed point (δ_0, Σ_0) , whose position is a function of the three system parameters: β , a , and J . For fixed a and β , there is a special value, J_c , of the bias current above which the superconducting state is destroyed: for $J>J_c$ the system displays periodic voltage oscillations. The threshold J_c can be readily computed numerically or analytically,⁸ in good agreement with experiment. Close to the bifurcation point, the system encounters a ‘‘bottleneck’’ once each period near the point where the stable (node) fixed point annihilates with an unstable (saddle) fixed point. The term ‘‘saddle-node connec-

tion’’ refers to the existence of orbits connecting each node to a saddle and each saddle to the next node. When the bifurcation occurs, a running state is created in a global bifurcation, the attractor resulting from the chain of (merged) saddle-node-saddle connections. The ensuing oscillations having the form of relaxation oscillations.⁷

The resulting oscillation frequency is generally very high, so that usually only the time-averaged quantity \bar{I}_s is measured in experiments (see, however, Ref. 14, where the oscillations were actually observed and the frequency computed in the extreme limiting case of $\beta\ll 1$). The SQUID response can be defined via an \bar{I}_s vs Φ_{ex} transfer characteristic and quantified in the oscillatory regime through a computation of the input-output gain or the output signal-to-noise ratio (SNR) at the frequency of a weak injected signal, as a function of the bias parameters (J, Φ_{ex}) .^{4,8} As emphasized above, the optimal response (highest gain or output SNR) is obtained just beyond the onset of oscillations. In what follows, our goal is to determine the spontaneous oscillation period in this regime. As we show, the result has a simple scaling form and compares well with direct numerical simulations of the full nonlinear equations (1).

The calculation proceeds in three steps. First, we consider the singular point at $J=J_c$, and determine the center manifold. Second, we unfold the dynamics for values of J close to J_c to generate the local nonlinear dynamics along the center manifold. Crucially, this local analysis captures the very slow dynamics which is responsible for the long period of the running state. Third, we get a quantitative expression for the running period by solving the reduced equation. The result is increasingly accurate as $J\rightarrow J_c$.

We start by considering the dynamics in the vicinity of the fixed-point solution when $J=J_c$. We introduce the small quantities $x=\delta-\delta_0$ and $y=\Sigma-\Sigma_0$ and Taylor expand the vector field to quadratic order,

$$\dot{x} = -\left(\frac{2}{\beta} + A\right)x + By + Cx^2 + 2Dxy + Cy^2 + O(3),$$

$$\dot{y} = -Ay + Bx + Dy^2 + 2Cxy + Dx^2 + O(3), \quad (2)$$

where $A = \cos\Sigma_0 \cos\delta_0$, $B = \sin\delta_0 \sin\Sigma_0$, $C = \frac{1}{2} \sin\delta_0 \cos\Sigma_0$, and $D = \frac{1}{2} \cos\delta_0 \sin\Sigma_0$, and $O(3)$ represents terms of cubic order and higher. A simple rotation \mathbf{S} diagonalizes the linear part

$$\mathbf{S} \begin{pmatrix} x \\ y \end{pmatrix} = \begin{pmatrix} u \\ v \end{pmatrix}; \quad \mathbf{S} = \begin{pmatrix} \cos\theta & \sin\theta \\ -\sin\theta & \cos\theta \end{pmatrix}, \quad (3)$$

where $\tan 2\theta = -\beta \sin\delta_0 \sin\Sigma_0$, so that

$$\frac{d}{dt} \begin{pmatrix} u \\ v \end{pmatrix} = \begin{pmatrix} \lambda & 0 \\ 0 & 0 \end{pmatrix} \begin{pmatrix} u \\ v \end{pmatrix} + \mathbf{S} \begin{pmatrix} Cx^2 + 2Dxy + Cy^2 \\ Dy^2 + 2Cxy + Dx^2 \end{pmatrix}, \quad (4)$$

where $\lambda = -2/\beta - 2 \cos\Sigma_0 \cos\delta_0$. To linear order, therefore, the trajectories relax to $u=0$ with exponential rate λ while the v evolution is neutral. The center manifold is determined by setting $du/dt=0$ and solving the resulting algebraic equation for $u(v)$.

We can repeat the same steps close to, but not precisely at, the bifurcation point. Technically,¹⁰ we treat the aug-

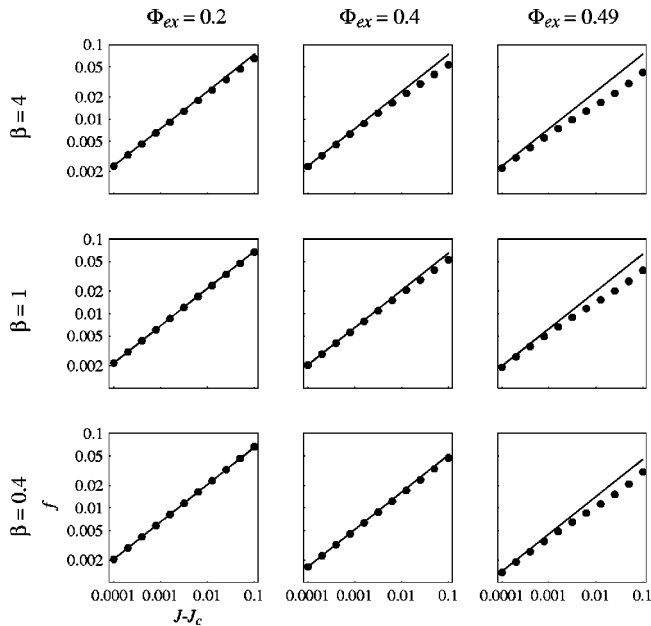


FIG. 2. Log-log plot of oscillation frequency $f \equiv 1/T$ vs $J - J_c$ determined from direct numerical simulations (points) and the analytic prediction Eq. (8) (line), for various values of β , Φ_{ex} , and J . Figure 1 was drawn for the same parameters as the middle left panel.

mented dynamical system, adding the equation $dJ/dt=0$ to Eq. (1), and expand the dynamics about the critical fixed point $(\delta_0, \Sigma_0, J_c)$. The resulting u - v subsystem (4) is modified only by a new constant term:

$$\frac{d}{dt} \begin{pmatrix} u \\ v \end{pmatrix} = \mathbf{S} \begin{pmatrix} 0 \\ J - J_c \end{pmatrix} + \begin{pmatrix} \lambda & 0 \\ 0 & 0 \end{pmatrix} \begin{pmatrix} u \\ v \end{pmatrix} + \mathbf{S} \begin{pmatrix} Cx^2 + 2Dxy + Cy^2 \\ Dy^2 + 2Cxy + Dx^2 \end{pmatrix}, \quad (5)$$

where $J - J_c$ is of order x^2 . It follows that $\dot{u} = \lambda u + O(2)$, so that the attracting subspace is $u = O(2)$, and the evolution of v on the center manifold is given by

$$\dot{v} = (J - J_c) \cos \theta + \alpha v^2 + O(3), \quad (6)$$

where the constant α is readily determined by carrying out the matrix multiplication indicated in Eq. (5), with result $\alpha = -\sin \theta (C - D \sin 2\theta) + \cos \theta (D - C \sin 2\theta)$. Ignoring terms of cubic order and higher, we may now integrate Eq. (6) directly, realizing that the dynamics (for small $J - J_c$) is dominated by the passage through the ‘‘bottleneck’’ where \dot{v} is at its smallest. We obtain the solution,

$$v(t) = \sqrt{\frac{F}{\alpha}} \tan(\sqrt{F\alpha} t) \quad (7)$$

with $F \equiv (J - J_c) \cos \theta$, whence the period T of the oscillations is¹⁵

$$T = \pi / \sqrt{F\alpha}. \quad (8)$$

Figure 2 compares this with numerical simulations of the full nonlinear dynamics given by Eq. (1). The simulations were run for a range of system parameters β and Φ_{ex} : owing to a parameter symmetry the full range of Φ_{ex} is between 0 and 0.5; meanwhile, practical SQUID’s are often fabricated to have $\beta \approx 1$. In the figure, the solid line represents Eq. (8), and the data are plotted over three decades in the reduced parameter $J - J_c$. In a typical SQUID, $J - J_c = 0.001$ might correspond to $\sim 5 - 10$ nA, with the oscillation frequency being in the GHz regime.⁴ The agreement is good over the full range shown; it is excellent for smaller values of β and Φ_{ex} . The agreement grows systematically worse for larger β and Φ_{ex} , since either reduces the size of the bottleneck regime. Even in the latter cases, the agreement improves in the limit $J \rightarrow J_c$, i.e., close enough to the bifurcation point, where the SQUID yields its optimal response to weak target signals in the presence of a noise floor. In this regime, the computed \bar{I}_s vs Φ_{ex} transfer characteristic agrees remarkably well with experimentally obtained ones.^{4,8}

In laboratory settings, it is often convenient to use the applied dc flux as the control parameter. We can easily arrive at the analogous result to Eq. (8) by keeping J fixed, and sweeping Φ_{ex} through its critical value Φ_{exc} at the bifurcation. This simply modifies the prefactor of Eq. (8), so T scales with the same exponent in $\Phi_{ex} - \Phi_{exc}$.

The above calculation represents a critical step towards *exploiting* the nonlinear response of the dc SQUID in the oscillatory regime. In our experiments⁴ the SQUID is operated as a free-running nonlinear dynamic device, not in the conventional flux-locked mode; hence, one is in a position to observe and exploit the richness of nonlinear dynamic behavior that would otherwise be inaccessible. In one application, the presence of an additional unknown ‘‘target’’ signal can be quantified by observing its effect on the free-running SQUID: a dc signal will shift the oscillation frequency, while a periodic signal will also generate combination tones in the power spectrum. A rather different effect can be used to dynamically suppress the low-frequency noise background in the SQUID itself, by injecting a *known* bias signal close to the running frequency and inducing a frequency locked state.¹⁶ Given the problems associated with operating in noisy/unshielded environments, this procedure could represent a major step in the active research area of noise cancellation. Investigations into these and other related topics must begin with an analysis of the effects of noise on the onset and frequency of the spontaneous oscillations.

Our calculation relied on a global phase-space structure, namely the saddle-node connection. While oscillatory behavior arising from this structure is rare in some general mathematical sense,⁹ it arises here from the fact that the Josephson variables are phase angles. A similar structure appears frequently in the class of coupled oscillator systems known as phase models. Thus, the treatment used in this paper should find wider application in, for instance, certain excitable biological oscillators and switches.¹⁷

A.R.B. and M.E.I. acknowledge support from the Office of Naval Research and an Internal Research grant at SPAWAR Systems Center. K.W. acknowledges summer support at SPAWAR through ONR/ASEE and support from ONR Grant No. N00014-99-1-0592.

- *Electronic address: kw2@prism.gatech.edu
 †Electronic address: bulsara@spawar.navy.mil
 ‡Electronic address: inchiosa@spawar.navy.mil
- ¹See, e.g., P.H. Bryant, R. Movshovich, and B. Yurke, *Phys. Rev. Lett.* **66**, 2641 (1991); K. Wiesenfeld and N.F. Tufillaro, *Physica D* **26**, 321 (1987); B. Derighetti, M. Ravani, R. Stoop, P. Meier, P. Brun, and R. Badii, *Phys. Rev. Lett.* **55**, 1746 (1985); G. Ahlers, M.C. Cross, P.C. Hohenberg, and S. Safran, *J. Fluid Mech.* **110**, 297 (1981), respectively.
- ²M.J. Feldman, P.T. Parrish, and R.Y. Chiao, *J. Appl. Phys.* **46**, 4031 (1975); S.T. Vohra, L. Fabiny, and K. Wiesenfeld, *Phys. Rev. Lett.* **72**, 1333 (1994).
- ³For overviews see K. Wiesenfeld and F. Moss, *Nature (London)* **373**, 33 (1995); A. Bulsara and L. Gammaitoni, *Phys. Today* **49** (3), 39 (1996); L. Gammaitoni, P. Hänggi, P. Jung, and F. Marchesoni, *Rev. Mod. Phys.* **70**, 1 (1998).
- ⁴A. Hibbs, in *Applied Nonlinear Dynamics and Stochastic Systems Near the Millenium*, AIP Conf. Proc. No. 411, edited by J. Kadtke and A. Bulsara (AIP, New York, 1997); A. Hibbs and B. Whitecotton, *Appl. Supercond.* **6**, 495 (1999); M. Inchiosa, A. Bulsara, A. Hibbs, and B. Whitecotton, *Phys. Rev. Lett.* **80**, 1381 (1998).
- ⁵For a good overview see, e.g., J. Clarke, *SQUIDS: Theory and Practice*, in *The New Superconducting Electronics*, edited by H. Weinstock and R. Ralston (Kluwer Publishers, Amsterdam, 1993).
- ⁶A. Barone and G. Paterno, *Physics and Applications of the Josephson Effect* (J. Wiley, New York, 1982); K. Likharev, *Dynamics of Josephson Junctions and Circuits* (Gordon and Breach, Philadelphia, 1984).
- ⁷H. Koch, in *Sensors, A Comprehensive Survey*, edited by W. Gopel, J. Hesse, and J. Zemel (VCH Publishers, Inc., New York, 1989), Vol. 5.
- ⁸M. Inchiosa, A. Bulsara, K. Wiesenfeld, and L. Gammaitoni, *Phys. Lett. A* **252**, 20 (1999); M. Inchiosa and A. Bulsara, in *Stochastic and Chaotic Dynamics in the Lakes*, AIP Conf. Proc. No. 502, edited by D.S. Broomhead, E. Luchinskaya, P.V.E. McClintock, and T. Mullin (AIP, NY, 2000), p. 583.
- ⁹J. Guckenheimer and P. Holmes, *Nonlinear Oscillations, Dynamical Systems, and Bifurcations of Vector Fields* (Springer-Verlag, New York, 1983).
- ¹⁰J.D. Crawford, *Rev. Mod. Phys.* **63**, 991 (1991).
- ¹¹A. Matsinger, R. de Bruyn Ouboter, and H. van Beelen, *Physica B & C* **94**, 91 (1978); C. Tesche, *J. Low Temp. Phys.* **44**, 119 (1981); E. Ben-Jacob, D. Bergman, Y. Imry, B. Matkowsky, and Z. Schuss, *J. Appl. Phys.* **54**, 6533 (1983); T. Ryhanen, H. Seppa, R. Ilmonemi, and J. Knuutila, *J. Low Temp. Phys.* **76**, 287 (1989).
- ¹²Y. Imry and L. Schulman, *J. Appl. Phys.* **49**, 749 (1978); E. Ben-Jacob and Y. Imry, *ibid.* **52**, 6806 (1981); P. Carelli and G. Paterno, in *Principles and Applications of Superconducting Quantum Interference Devices*, edited by A. Barone (World Scientific, Singapore, 1992).
- ¹³R.L. Peterson and D.G. McDonald, *J. Appl. Phys.* **54**, 992 (1983).
- ¹⁴K. Nakajima *et al.* *J. Appl. Phys.* **60**, 3786 (1986).
- ¹⁵One may by inspection write down an alternate normal form $\dot{v} = F + 2\alpha(1 - \cos v)$ that yields bounded solutions [unlike Eq. (7)] and agrees with Eq. (6) to $O(2)$. This normal form yields the period $T = 2\pi / \sqrt{F^2 + 4F\alpha}$ which reduces to Eq. (8) for $F \ll 4\alpha$.
- ¹⁶K. Wiesenfeld and I. Satija, *Phys. Rev. B* **36**, 2483 (1987).
- ¹⁷See, e.g., J.D. Murray, *Mathematical Biology* (Springer-Verlag, Berlin, 1989).